



**HAL**  
open science

## Discrete motor imageries can be used to allow a faster detection

Sébastien Rimbart, Oleksii Avilov, Laurent Bougrain

► **To cite this version:**

Sébastien Rimbart, Oleksii Avilov, Laurent Bougrain. Discrete motor imageries can be used to allow a faster detection. 7th Graz Brain-Computer Interface Conference 2017, Sep 2017, Graz, Austria. hal-01512407

**HAL Id: hal-01512407**

**<https://inria.hal.science/hal-01512407>**

Submitted on 22 Apr 2017

**HAL** is a multi-disciplinary open access archive for the deposit and dissemination of scientific research documents, whether they are published or not. The documents may come from teaching and research institutions in France or abroad, or from public or private research centers.

L'archive ouverte pluridisciplinaire **HAL**, est destinée au dépôt et à la diffusion de documents scientifiques de niveau recherche, publiés ou non, émanant des établissements d'enseignement et de recherche français ou étrangers, des laboratoires publics ou privés.

# DISCRETE MOTOR IMAGERIES CAN BE USED TO ALLOW A FASTER DETECTION

Sébastien Rimbart<sup>1,2,3</sup>, Oleksii Avilov<sup>4,1,2,3</sup>, and Laurent Bougrain<sup>2,1,3</sup>

<sup>1</sup>Neurosys team, Inria, Villers-lès-Nancy, F-54600, France

<sup>2</sup>Artificial Intelligence and Complex Systems, Université de Lorraine, LORIA, UMR 7503, Vandœuvre-lès-Nancy, F-54506, France

<sup>3</sup>Neurosys team CNRS, LORIA, UMR 7503, Vandœuvre-lès-Nancy, F-54506, France

<sup>4</sup>Electronic Dept., National Technical University of Ukraine "Igor Sikorsky Kyiv Polytechnic Institute", Kyiv, Ukraine

E-mail: sebastien.rimbart@inria.fr

**ABSTRACT:** Motor imagery (MI) modifies the neural activity within the primary sensorimotor areas of the cortex and can be measured through the analysis of electroencephalographic (EEG) recordings. It is particularly interesting for Brain-Computer Interface (BCI) applications. In most MI-based BCI experimental paradigms, subjects realize continuous motor imagery (CMI), i.e. a repetitive and prolonged intention of movement, for a few seconds. The system detects the movement based on the *event-related desynchronization* and the *event-related synchronization* features in electroencephalographic signal. Currently, improving efficiency such as detecting faster a motor imagery is an important issue in BCI to avoid fatigue and boredom. The purpose of this study is to show the difference, in term of classification, between a discrete motor imagery, i.e. a single short MI, and a CMI. The results of experiments involving 16 healthy subjects show that a BCI based on DMI is as effective as a BCI based on CMI and could be used to allow a faster detection.

## INTRODUCTION

Motor imagery (MI) is the ability to imagine performing a movement without executing it [1]. According to Jeannerod [2], MI represents the result of conscious access to the content of the intention of a movement, which is usually performed unconsciously during movement preparation [3]. MI has two different components, namely the visual-motor imagery and the kinesthetic motor imagery (KMI) [4]. KMI generates an *event-related desynchronization* (ERD) and an *event-related synchronization* (ERS) in the contralateral sensorimotor area, which is similar to the one observed during the preparation of a real movement (RM) [5]. More precisely, compared to a resting state taken before a motor imagery, several power modulations are observed in the alpha (8-12 Hz) and in the beta (18-25 Hz) bands of the electroencephalographic signal measured over the sensorimotor area corresponding to the body part involved in the motor imagery. Firstly

there is a gradual power decrease in the alpha and in the beta bands, called ERD. Secondly, a low power level is maintained during the movement. Finally, from 300 to 500 milliseconds after the end of the motor imagery, there is a power increase called ERS or post-movement beta rebound with a duration of about one second. Although several studies showed an activity uniquely in the contralateral area [6], other studies showed that ERD and ERS are also in the ipsilateral area [7].

Emergence of ERD and ERS patterns during and after a MI has been intensively studied in the *Brain-Computer Interface* (BCI) domain [8] in order to define detectable commands for the system. Hence, a better understanding of these processes could allow for the design of better interfaces between the brain and a computer system. Additionally, they could also play a major role where MI are involved such as rehabilitation for stroke patients [9], monitoring consciousness during general anesthesia [10] or the recovery of the motor capacity after neurological damage. For example MI training is a promising approach in facilitating paretic limb recovery.

Currently, most of the paradigms based on MIs require the subject to perform the imagined movement several times for a predefined duration of a few seconds. In this study, such a task is commonly referred to as a continuous motor imagery (CMI). However, first the duration of the experiment is long. Second a succession of flexions and extensions generate an overlapping of ERD and ERS patterns making the signal less detectable. In fact, one simple short MI, referred in this article as a discrete motor imagery (DMI), could be more useful for two reasons. Firstly, a DMI could be used to combat fatigue and boredom for BCI users improving ERD and ERS production [11]. Secondly, the ERD and ERS generated by the DMI could be detectable at a higher quality and more rapidly compared to a CMI. This was found in a previous study that established a relationship between the duration of the MI and the quality of the ERS extracted [12]. It also showed that a brief MI (i.e. a 2-seconds MI) could be more efficient than a sustained MI. Our main hypothe-

sis is that a DMI generates robust ERD and ERS patterns which could be detectable by a BCI system. Results indicate that a DMI produces a robust ERS and is as detectable as a CMI.

## MATERIALS AND METHODS

**Participants:** 16 right-handed healthy volunteer subjects took part in this experiment (9 men and 7 women, from 19 to 43 years old). They had no medical history which could have influenced the task such as diabetes, peripheral neuropathology, renal insufficiency, anti-depressant treatment or motor problem. All subjects gave their agreement and signed an information consent form approved by the ethical INRIA committee before participating. This experiment follows the statements of the WMA declaration of Helsinki on ethical principles for medical research involving human subjects [13].

**Real movement:** The first task consisted of an isometric flexion of the right index finger on a computer mouse. A low frequency beep indicated when the subject had to execute the task. The right-click is recorded as a trigger and has allowed to know exactly when the participant executes the RM.

**Discrete imagined movement:** The second task was a DMI of the previous real movement. A low frequency beep indicated when the subject has to execute the task.

**Continuous imagined movement:** The third task was a CMI during four seconds of the real movement of the first task. More precisely, the subject imagined several (around four) flexions and extensions of the right index finger. This way, the DMI differed from the CMI by the repetition of the imagined movement. For this task, two beeps, respectively with low and high frequencies, separated by a four second delay, indicated the beginning and the end of the CMI.

**Protocol:** Each of the three tasks introduced in section corresponds to a session. The subjects completed three sessions during the same day. All sessions were split into several runs. Breaks of a few minutes were planned between sessions and between runs to avoid fatigue. Before each session, the task was described, and the subject practiced the tasks. At the beginning of each run, the subject was told to relax for 30 seconds. Condition 1 corresponded to RMs was split into 2 runs of 50 trials. Conditions 2 and 3 corresponded to discrete and continuous imagined movements, respectively, was split into 4 runs of 25 trials. Thus, 100 trials were performed by subjects for each task. Each experiment began with condition 1 as session 1. Conditions 2 and 3 were randomized to avoid possible bias cause by fatigue, gel drying or another confounding factor. For conditions 1 and 2, the timing scheme of a trial was the same: one low frequency beep indicated the start followed by a rest period of 12 seconds. For condition 3, a low frequency beep indicated the start of the MI to do during 4 seconds, followed by a rest period of 8 seconds. The end of the MI is announced by a high frequency beep (Fig. 1).

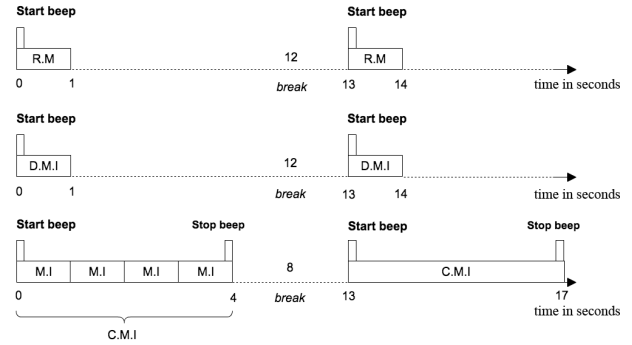


Figure 1: Timing schemes of a trial for each task: Real Movement (RM, top); Discrete Motor Imagery (DMI, middle); Continuous Motor Imagery (CMI, bottom). The DMI and CMI sessions are randomized.

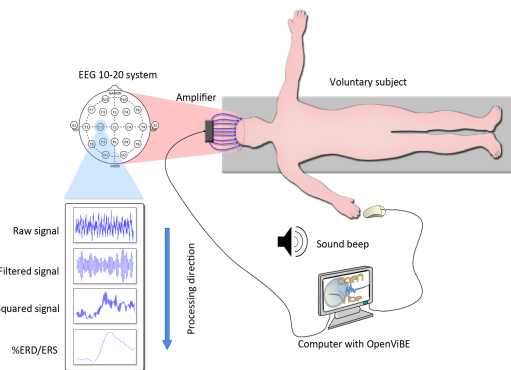


Figure 2: Schematic representation of the experiment. A low frequency beep indicates the start of the (real or imagined) movement. A high frequency beep indicates the end of the continuous imagined movement. Depending on the task, the subject presses or imagines pressing the button of the mouse.

**Behavioral data:** A custom-written scenario for OpenViBE [14] was designed to automate the generation of beeps, and to record triggers and EEG signals. The triggers corresponding to the right-click allowed us to detect potential behavioral errors. All non realized movements were removed from the analysis. For all three tasks, we used a fixed preparatory period duration in which the subjects could anticipate the GO signal.

**EEG data:** EEG signals were recorded through the OpenViBE platform with a commercial REFA amplifier developed by TMS International. The EEG cap was fitted with 9 passive electrodes re-referenced with respect to the common average reference across all channels over the extended international 10-20 system positions to cover the primary sensorimotor cortex. The selected electrodes are FC3, C3, CP3, FCz, Fz, CPz, FC4, C4, CP4. No additional filtering was used during the recording. Skin-electrode impedances were kept below 5 k $\Omega$ . Incorrect trials were removed from the analyses.

**ERD/ERS patterns:** To evaluate more precisely the modulation produced by the tasks, we computed the

ERD/ERS% using the “band power method” [5] with a matlab code. First, the EEG signal is filtered between 8-30 Hz (Alpha+Beta) for all subjects using a 4th-order Butterworth band-pass filter. Then, the signal is squared for each trial and averaged over trials. Then it is smoothed using a 250-millisecond sliding window with a 100 ms shifting step. We have chosen a specific sliding window because the nature of the real and imagined movement, as well as the components ERD/ERS that underline them, require a short window. Finally, the averaged power computed for each window was subtracted and then divided by the averaged power of a baseline corresponding to 2 seconds before each trial. Finally, the averaged power computed for each window was subtracted and then divided by the averaged power of a baseline corresponding 2 seconds before each trial. This transformation was multiplied by 100 to obtain percentages. This process can be summarized by the following equation:

$$ERD/ERS\% = \frac{\overline{x^2} - \overline{BL^2}}{\overline{BL^2}} \times 100, \quad (1)$$

where  $\overline{x^2}$  is the average of the squared signal over all trials and samples of the studied window,  $\overline{BL^2}$  is the mean of a baseline segment taken at the beginning of the corresponding trial, and ERD/ERS% is the percentage of the oscillatory power estimated for each step of the sliding window. It is done for all channels separately.

ERD and ERS are difficult to observe from the EEG signal. Indeed, an EEG signal expresses the combination of activities from several neuronal sources. One of the most effective and accurate techniques used to extract events is the average technique [15]. We decided to use this technique to represent the modulation of power of the Alpha+Beta rhythms for three tasks (Real Movement, Discrete Motor Imagery and Continuous Motor Imagery).

*Common Spatial Pattern:* We used the algorithm called Common Spatial Pattern (CSP) to extract motor imagery features from EEG signals; this generated a series of spatial filters that were applied to decompose multi-dimensional data into a set of uncorrelated components [16]. These filters aim to extract elements that simultaneously maximize the variance of one class, while minimizing the variance of the other one.

*Feature extraction and linear discriminant analysis:* We trained a linear discriminant classifier to distinguish the features of motor imageries from the ones of a resting state. We applied the common spatial pattern algorithm to obtain 3 pairs of linear combinations from the 8-30 Hz filtered EEG signals. Then for each linear combinations we computed the logarithm of the variance for a studied window. We considered a 2 seconds window taken 3 seconds before the GO signal for the resting state. The 1 second window before the GO signal is not taken into consideration because the beep can generate an audio ERP and the subject usually prepares the movement in advance. So it not really a resting state. The features of a DMI is computed from 0.2 to 1 second after the GO signal (Fig. 5,

Tab. 1). The features of a CMI is computed from 0.2 to 3 seconds after the GO signal (Fig. 5, Tab. 1).

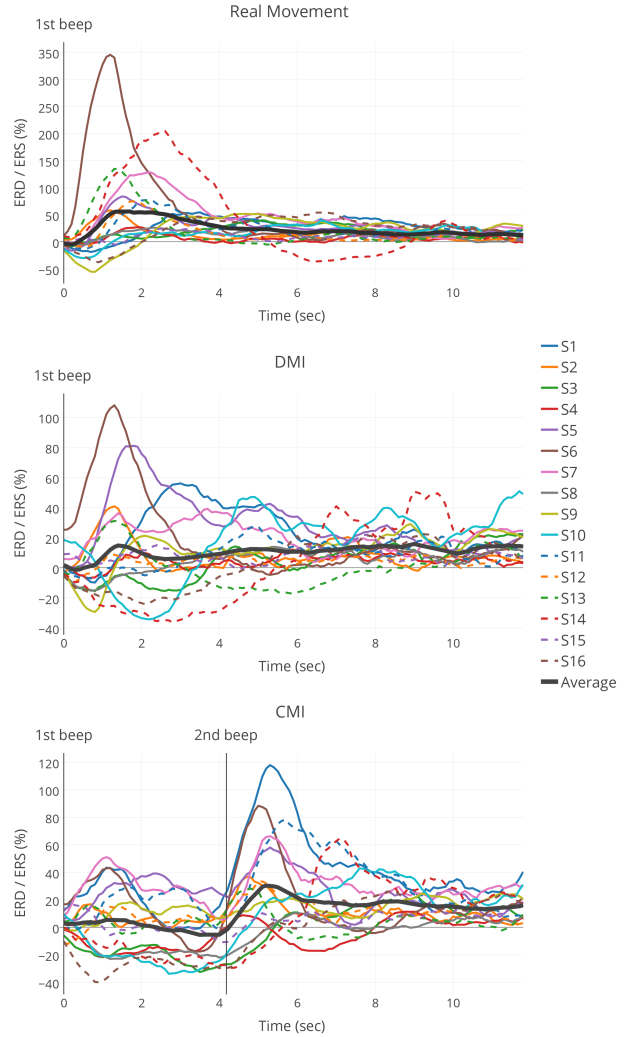


Figure 3: Grand average ERD/ERS% curves (in black, Average) estimated for the RM, the DMI and the CMI within the alpha + beta band (8-30 Hz) for electrode  $C_3$ . The average for each subject is also presented. A first beep indicated the start of the (real or imagined) movement. A second beep indicated the end of the continuous imagined movement.

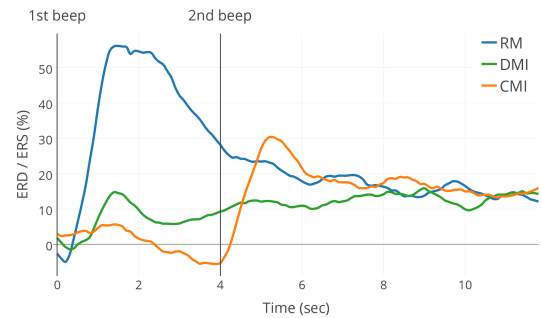


Figure 4: Grand average ERD/ERS% curves estimated for the RM (blue), the DMI (green) and the CMI (orange)

within the alpha + beta band (8-30 Hz) for electrode  $C_3$ . A first beep indicated the start of the (real or imagined) movement. A second beep indicated the end of the continuous imagined movement.

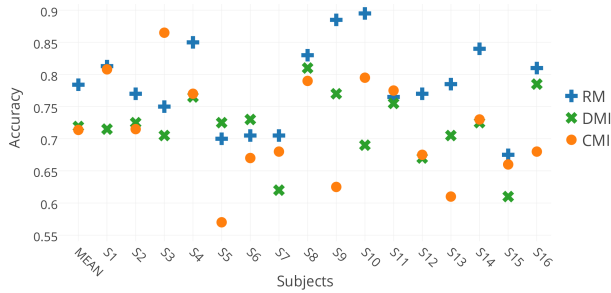


Figure 5: Accuracies obtained by linear discriminant analyses for the 3 conditions (RM, CMI and DMI). The features of a RM and DMI are computed from 0.2 to 1 second after the GO signal. The features of a CMI are computed from 0.2 to 3 seconds after the GO signal.

Table 1: Grand average accuracies obtained by linear discriminant analyses for the 3 conditions (RM, CMI and DMI) and 3 frequency bands (alpha, beta and alpha + beta).

	Frequency Bands		
	Alpha	Beta	Alpha+Beta
	8-12 Hz	18-25 Hz	8-30 Hz
<b>RM</b>	75,3 ± 6,17	73,8 ± 6,1	<b>78,4 ± 6,67</b>
<b>DMI</b>	70,4 ± 5,5	71,2 ± 3,6	71,9 ± 5,4
<b>CMI [0.2-3s]</b>	68,8 ± 5,6	71,2 ± 6	71,4 ± 8,15
<b>CMI [0.2-1s]</b>	68,1 ± 5,25	68,4 ± 5,8	70,625 ± 6,1

## RESULTS

To prove the usability of a DMI in BCI-domain, firstly we computed ERD and ERS patterns to study the relative power (8-30 Hz) for the electrode C3. Secondly, we verified the detectability of a DMI in calculating classification rate.

*ERD and ERS modulation:* To verify if a DMI generates ERD and ERS patterns which could be detectable by a CMI, we studied the relative power (8-30 Hz) for the electrode C3. Electrode C3 is suitable for monitoring right hand motor activity. A grand average was calculated over the 16 subjects. We used a Friedman’s test to analyze whether ERS were significantly and respectively different during the three conditions. Due to eyes-closed experiment, the alpha band is disturbed (confirmed by the time-frequency analysis) and not considered for this study. Consequently values corresponding to the desynchronization during the real and imagined movements will appear smaller. Moreover a visual inspection of time-frequency analysis shown modulations of alpha + beta power between 8-30 Hz for all the 16 subjects (Fig. 3).

*ERD and ERS modulation during/after a real movement:* The ERD/ERS% averages (Fig. 4) indicate that one second after the cue, the power in the 8-30 Hz band increases by around 60%, reaches its maximum and returns to the baseline 7 seconds after. The evolution from ERD to ERS is rapid (less than one second) and should be linked to the type of movement realized by the subjects. Interestingly, each subject (except Subject 9 and Subject 16) has the same ERD/ERS% profile (i.e. a strong rebound) after the real movement (Fig. 3).

*ERD and ERS modulation during/after a discrete motor imagery:* The ERS post-DMI reaches 18% which is weaker compare to the other tasks (Fig. 4). Some subjects (S1, S2, S5, S6, S10) have a stronger robust ERS produced by DMI while others have no beta rebound. Some subjects (S9, S10, S15) have a strong ERD after the task (Fig. 3). This variability between subjects could explain the weakness of the ERS post-DMI. The presence of ERD and ERS during/after a DMI suggest that a DMI could be used in BCI-domain.

*ERD and ERS modulation during/after a continuous motor imagery:* During the CMI, the subjects imagined several movements in a time window of 4 seconds. Fig. 4 shows a global decrease of activity during the CMI and stronger modulation in 8-30 Hz after the CMI. The results of the grand average shows a low desynchronization during this time window. It is interesting to note that some subjects (S7, S9, S11) have no desynchronization during the CMI task and could have a negative effect on the classification phase. Other subjects (S2, S15) have a different profile which shows that a first ERS is reached one second after the beginning of the CMI, then the power increases and decreases again, being modulated during 3 seconds. Indeed, this global ERD can be considered as the concatenation of several ERDs and ERSs due to the realization of several MIs. The variability between subjects during this period could also have a negative effect on the classification rate.

*Detection results:* Discrete motor imageries generate robust ERD and ERS (see previous section). In this section, we will study if they are detectable enough to have a faster detection in BCI than using continuous motor imageries. For each subject, 4 runs of 25 trials were available. The process of the cross validation consisted in using trials of 3 runs for train classifier and 1 run for test it. Four permutations were possible and we averaged accuracies obtain by the 4 classifiers on their testing run for a better evaluation. This method of cross validation was chosen because of its proximity to online condition. Figure 5 presents the accuracy for each subject and the mean accuracy. The mean accuracy for RM, DMI and CMI are respectively 78,4%, 71,9% and 71,4%. The detection of real movement is easier than the one of motor imageries. The difference between the two motor imageries is not statistically significant at a level of 5%. The precision of the ME is 0,78 (22% of false positive) and the recall is 0.79. The precision of the DMI is 0.71 (29% of false positive) and the recall is 0.74. The precision of the CMI

is 0,73 (27% of false positive) and the recall is 0,68. Interestingly, some subjects (S5, S6, S9, S16) have a better detection for the DMI task. In Tab. 1, we computed the grand average of accuracies for the three conditions (RM, DMI and CMI) for three frequency bands (alpha, beta and alpha + beta). It appears that the 8-30 Hz frequency band increases the classification rate. Furthermore, the comparison of the classification rate between a DMI and a CMI on the same period (0.2s-1s) shows an equivalence.

## DISCUSSION

The subjects carried out voluntary movements, DMI and CMI of an isometric flexion of the right hand index finger. Results show that the power in the 8-30 Hz band is modulated during the three tasks. The comparison between ERSs suggests that subjects on average have a stronger ERS during a CMI than a DMI. However, this is not the case for all subjects. Furthermore, the detection rate for a DMI is as effective as for a CMI.

*EEG system:* It is well established that a large number of electrodes allows having a good estimation of the global average potential of the whole head [17]. Although we focused on specific electrodes, our results were similar by using method of the derivation, which corresponded with the literature. We chose to study C3 without derivation because we are interested in designing a minimal system to detect ERD and ERS during general anesthesia conditions.

*ERD/ERS modulation during real movements:* The results are coherent with previous studies describing ERD/ERS% modulations during motor actions. The weakness of the ERD can be linked to the instruction that was focused more on the precision than the speed of the movement [18]. However, although some subjects were making efforts to do a voluntary movement, we must consider that an isometric flexion movement on a mouse is a movement setting in the subject's memory. This can have an impact on the low ERD amplitude. We also showed that the rebound starts before the click. Since a mouse click, is a really fast movement, we expect that the beta rebound will appear fast as well [19].

*ERS modulation during motor imageries:* The results show that the ERS is lower after a DMI or a CMI than after a real movement, which has been already been demonstrated previously [20]. However, the novelty is the beta rebound is stronger on average after a CMI than DMI for a few subjects.

*ERD modulation during continuous motor imagery:* When the subjects performed the CMI, the ERD was highly variable during the first 4 seconds. For some subjects, our hypothesis is there are some intern-ERD and intern-ERS into this period. The difficulty is that the CMI involves several MI, that are not synchronized across trials, unlike the DMI which starts and ends at roughly the same time for each trial, due to the cue. Normally, for continuous real movement, the ERD was sustained during the execution of this movement [21]. However, in

our data it is possible to detect several ERDs during the 4 seconds of CMI where the subject performed 4 MIs. This assumes that the ERD and ERS components overlap in time when we perform a CMI. Several studies already illustrate the concept of overlap of various functional processes constituting the beta components during RMs [22]. Moreover, the beta rebound generated by a median nerve stimulation is reduced when the stimulation is made during different types of real or imagined hand movements [23], [24]. However, even if the components cancel each other out in the signal, it does not mean that the operation of the underlying processes are similarly affected. This interpretation assumes implicitly that the components are combining each other, which means that the temporal superposition of an ERD and an ERS would result in an intermediate amplitude signal. This could explain why the ERD during a CMI could be less detectable and more varied than the ERD during a DMI. To validate this hypothesis, we plan to design a new study to explore how two fast-successive movements (or MIs) can affect the signal in the 8-30 Hz frequency band.

*Detection rate:* We showed that the detection of a real movement was easier than discrete and continuous motor imageries but we could discuss about the weakness of the classification rate for the three task. Usually, a real movement has often a high classification rate and it is not the case in this study. However, it is important to remind that the subject performed real movement, DMI and CMI of an isometric flexion of the right hand index finger. The rapidity and the precision of the three tasks could be linked with the low classification rate. One limitation of this study is that all trials of a type had the same length and was not randomized within a block.

*Establishing a link between the ERD/ERS users profiles and the detection rate:* Our study shows results which could allow to understand more differences, in term of ERD and ERS, between subjects. Indeed, we showed that for a same task (RM, DMI and CMI), for some subjects a strong ERS appeared whereas for some others, no ERS appeared. We observed the same phenomenon for ERD. It could be interesting to establish a link between the particular ERD/ERS users profiles and the detection rate. The importance of BCI users profiles, especially for patients with severe motor impairments has already been established by other studies [25]. This is why, we expect designing an adaptive BCI based on the specific motor activity of the motor cortex. More subjects are necessary to precise this BCI user profile.

## CONCLUSION

This article examined the modulation of power (8-30 Hz) in EEG during a real movement, a discrete motor imagery (DMI) and a continuous motor imagery (CMI). We showed that during a real voluntary movement corresponding to an isometric flexion of the right hand index finger a low ERD appeared, and was followed by a rapid and powerful ERS. Subsequently, we showed that

the ERD and ERS components were still modulated by both a DMI and a CMI. The ERS is present in both cases and shows that a DMI could be used in BCI domain. The classification results show no any difference between a CMI and a DMI and confirm that a DMI could have a future impact in BCI-domain to save time and avoid fatigue.

## REFERENCES

- [1] L. Avanzino, A. Giannini, A. Tacchino, E. Pelosin, P. Ruggeri, and M. Bove, "Motor imagery influences the execution of repetitive finger opposition movements, *Neuroscience Letters*, vol. 466, no. 1, pp. 11–15, 2009.
- [2] M. Jeannerod, "Mental imagery in the motor context, *Neuropsychologia*, vol. 33, no. 11, pp. 1419–32, Nov 1995.
- [3] M. Lotze and U. Halsband, "Motor imagery, " *JPhysiol Paris*, vol. 99, no. 4-6, pp. 386–95, Jun2006.
- [4] C. Neuper, R. Scherer, M. Reiner, and G. Pfurtscheller, "Imagery of motor actions: Differential effects of kinesthetic and visual motor mode of imagery in single-trial EEG, *Cognitive Brain Research*, vol. 25, no. 3, pp. 668 – 677, 2005.
- [5] G. Pfurtscheller and F. H. Lopes da Silva, "Event-related eeg/meg synchronization and desynchronization: basic principles, *Clin Neurophysiol*, vol. 110, no. 11, pp. 1842–57, Nov 1999.
- [6] G. Pfurtscheller and C. Neuper, "Motor imagery and direct brain-computer communication, *Proceedings of the IEEE*, vol. 89, no. 7, pp. 1123 –1134, July 2001.
- [7] S. Fok, R. Schwartz, M. Wronkiewicz, C. Holmes, J. Zhang, T. Somers, D. Bundy, and E. Leuthardt, "An eeg-based brain computer interface for rehabilitation and restoration of hand control following stroke using ipsilateral cortical physiology. *Conf Proc IEEE Eng Med Biol Soc*, vol. 2011, pp. 6277–6280, 2011.
- [8] E. W. W. Jonathan Wolpaw, Ed., *Brain-Computer Interfaces: Principles and Practice*. Oxford university press, 2012.
- [9] A. J. Butler and S. J. Page, "Mental practice with motor imagery: evidence for motor recovery and cortical reorganization after stroke. *Arch Phys Med Rehabil.* , vol. 87, pp. S2–11, dec. 2006.
- [10] Y. Blokland, J. Farquhar, J. Lerou, J. Mourisse, G. J. Scheffer, G.-J. van Geffen, L. Spyrou, and J. Bruhn, "Decoding motor responses from the eeg during altered states of consciousness induced by propofol, *Journal of Neural Engineering*, vol. 13, no. 2, p. 026014, 2016.
- [11] M. Ahn and S. C. Jun, "Performance variation in motor imagery brain-computer interface: a brief review. *J Neurosci Methods*, vol. 243, pp. 103–110, Mar 2015.
- [12] E. Thomas, J. Fruitet, and M. Clerc, "Investigating brief motor imagery for an erd/ers based bci. *Conf Proc IEEE Eng Med Biol Soc*, vol. 2012, pp. 2929–2932, 2012.
- [13] A. World Medical, "World medical association declaration of helsinki: ethical principles for medical research involving human subjects. *J Postgrad Med*, vol. 48, no. 3, pp. 206–208, Jul-Sep 2002, KIE:KIE Bib: human experimentation.
- [14] Y. Renard, F. Lotte, G. Gibert, M. Congedo, E. Maby, V. Delannoy, O. Bertrand, and A. Lécuyer, "Open-vibe: An opensource software platform to design, test and use brain-computer interfaces in real and virtual environments, *Presence : teleoperators and virtual environments*, vol. 10, no. 1, 2010.
- [15] R. Quiroga and H. Garcia, "Single-trial event-related potentials with wavelet denoising, *Clinical Neurophysiology*, vol. 114, no. 2, pp. 376–390, 2003.
- [16] B. Blankertz, R. Tomioka, S. Lemm, M. Kawanaba, and K. Muller, "Optimizing spatial filters for robust EEG single-trial analysis [revealing tricks of the trade], *IEEE Signal processing magazine*, 2008.
- [17] J. Dien, "Issues in the application of the average reference: review, critiques, and recommendations, " *Behavior Research Methods*, vol. 30, p. 34, 1998.
- [18] B. Pastotter, F. Berchtold, and K.-H. T. Bauml, "Oscillatory correlates of controlled speed-accuracy tradeoff in a response-conflict task, *Hum Brain Mapp*, vol. 33, no. 8, pp. 1834–49, Aug 2012.
- [19] L. M. Parkes, M. C. M. Bastiaansen, and D. G. Norris, "Combining eeg and fmri to investigate the post-movement beta rebound, *Neuroimage*, vol. 29, no. 3, pp. 685–96, Feb 2006.
- [20] A. Schnitzler, S. Salenius, R. Salmelin, V. Jousmaki, and R. Hari, "Involvement of primary motor cortex in motor imagery: a neuromagnetic study. *Neuroimage*, vol. 6, no. 3, pp. 201–208, Oct 1997.
- [21] N. Erbil and P. Ungan, "Changes in the alpha and beta amplitudes of the central eeg during the onset, continuation, and offset of long-duration repetitive hand movements. *Brain Res*, vol. 1169, pp. 44–56, Sep 2007.
- [22] B. E. Kilavik, M. Zaepffel, A. Brovelli, W. A. MacKay, and A. Riehle, "The ups and downs of beta oscillations in sensorimotor cortex. *Exp Neurol*, vol. 245, pp. 15–26, Jul 2013.
- [23] G. Pfurtscheller, M. Woertz, G. Muller, S. Wriessneger, and K. Pfurtscheller, "Contrasting behavior of beta event-related synchronization and somatosensory evoked potential after median nerve stimulation during finger manipulation in man. *Neurosci Lett*, vol. 323, no. 2, pp. 113–116, Apr2002.
- [24] S. Salenius, A. Schnitzler, R. Salmelin, V. Jousmaki, and R. Hari, "Modulation of human cortical rolandic rhythms during natural sensorimotor tasks, *NeuroImage*, vol. 5, no. 3, pp. 221–228, 1997.
- [25] J. Hohne, E. Holz, P. Staiger-Salzer, K.-R. Muller, A. Kubler, and M. Tangermann, "Motor imagery for severely motor-impaired patients: Evidence for brain-computer interfacing as superior control solution, *PLOS ONE*, vol. 9, 2014.